Takamichi YOSHIMOTO[1], Yasuyoshi ASAI[1], Katsuhiro HIRATA[1], Tomohiro OTA[2]

Osaka University (1), Panasonic Electric Works (2)

New Two-DOF Resonant Actuator Driven by Vector Control

Abstract. *This paper proposes a two-DOF resonant actuator that can be independently driven in two axes under vector control. Vector control is employed to control each drive axis independently by treating the field current element as the z-axis thrust element and the torque current element as the x-axis thrust element. The effectiveness of the actuator is verified by the experimental results of a prototype.*

Streszczenie. *Artykuł przedstawia aktuator rezonansowy z dwoma stopniami swobody, który może być niezależnie kierowany w dwóch osiach przez sterownik wektorowy. Sterowanie każdym kierunkiem może być niezależne poprzez traktowanie elementu prądowo-polowego jako osi z elementu siłowego, podczas gdy element prądowo-momentowy traktowany jest jako oś x elementu siłowego. Skuteczność aktuatora zweryfikowano w badaniach prototypu. (**Nowy z dwoma stopniami swobody aktuator rezonansowy kierowany poprzez sterownik wektorowy**).*

Keywords: two-dof, vector control, resonant actuator, Finite Element Method.
Słowa kluczowe: dwa stopnie swobody, aktuator rezonansowy, metoda elementów skończonych

Introduction

Linear resonant actuators (LRAs) have been used in a wide range of applications because they can reciprocate in a comparatively short stroke in spite of their compact size and light weight. We have proposed a coupled method for analyzing its dynamic characteristics under feedback control by combining the magnetic field, electric field, control method, and its motion into our 3-D FEM code [1]-[7].

Recently, multi-degree of freedom actuators have been attracting attention[8-9], and we have also been developing various kinds of two-DOF resonant actuators [10-12]. However, these actuators have no drive axis in the direction of the air gap because of control difficulty.

This paper proposes a new two-DOF resonant actuator that can be independently driven in the x-axis and z-axis (air gap direction) under vector control. The performance of the actuator is verified with a prototype.

Basic Structure of the Actuator

The basic structure of the two-DOF resonant actuator is shown in Fig. 1. This actuator mainly consists of a mover, a stator and resonance springs in the x and z directions that support the mover. The mover is composed of permanent magnets (NbFeB, Br=1.4T) fixed on a back yoke. The stator is composed of an E-shaped laminated yoke with three excitation coils (45 turns). This actuator is assumed to move with a range of ±1.2mm in the x-direction and ±0.5mm in the z-direction, respectively.

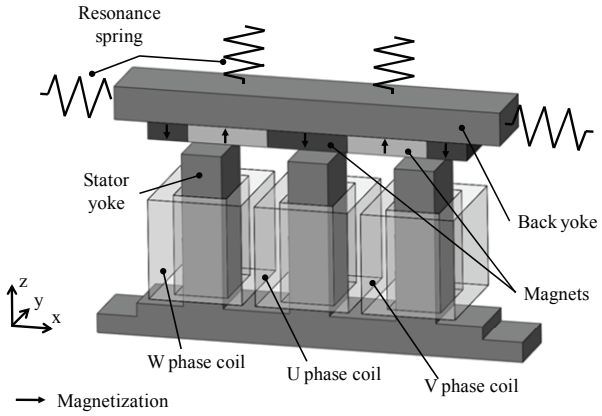

Fig.1. Structure of two-DOF resonant actuator

Vector control

This actuator is controlled by vector control. Vector control is commonly used for advanced control of a rotating machine. By using this type of control, it becomes easier to treat the motor field element (d-axis) and torque element (q-axis) independently rather than controlling the UVW axes of the 3-phase current.

This actuator can operate in the x and z direction by treating the field current element (i_d element) as the z- axis thrust element and the torque current element (i_q element) as the x- axis thrust element. This actuator is a non-salient pole type and the thrust equation under vector control is given as follows:

$$\begin{bmatrix} F_z \\ F_x \end{bmatrix} = \phi \begin{bmatrix} i_d \\ i_q \end{bmatrix} \tag{1}$$

where i_d and i_q are the currents of the d- and q- axis, and ϕ is the armature interlinkage flux from the permanent magnet. Fig. 2 shows correspondence of the coordinate system of a rotating machine and this actuator. The x-y axis is the coordinate system fixed to stator, and the d-q axis is the coordinate system which moves with mover. The electric angle between the stator and the mover θ is given as follows:

$$\theta = \frac{x}{l}\pi \tag{2}$$

where *l* is the distance between the north and south poles. From equations (1) and (2), the current of each phase is calculated by d-q conversion. However, thrust can not be correctly controlled with vector control because of the influence of the edge effect. Therefore the current should be corrected by the following equation.

$$\begin{bmatrix} F_d^* \\ F_q^* \end{bmatrix} = \begin{bmatrix} \phi_{ux}(\theta) & \phi_{vx}(\theta) & \phi_{wx}(\theta) \\ \phi_{uz}(\theta) & \phi_{vz}(\theta) & \phi_{wz}(\theta) \end{bmatrix} \begin{bmatrix} \cos\theta & -\sin\theta \\ \cos(\theta - \frac{2}{3}\pi) & -\sin(\theta - \frac{2}{3}\pi) \\ \cos(\theta + \frac{2}{3}\pi) & -\sin(\theta + \frac{2}{3}\pi) \end{bmatrix} \begin{bmatrix} i_d \\ i_q \end{bmatrix} \tag{3}$$

where F_d^* and F_q^* are the target thrust of each axis, $\phi ux(\theta)$, $\phi vx(\theta)$, $\phi wx(\theta)$, $\phi uz(\theta)$, $\phi vz(\theta)$, $\phi wz(\theta)$ are the interlinkage magnetic flux from each phase coil on each axis. The target thrust is arbitrarily given, and i_d and i_q at each position are decided from equation (3).

Magnetic Field Analysis

Using the magnetic vector potential $\boldsymbol{A}$, and the current flowing through the coils I_0, the equations of the magnetic field and the electric circuit are coupled and are expressed as follows:

$$\mathrm{rot}(\nu\,\mathrm{rot}\,\boldsymbol{A}) = \boldsymbol{J}_0 + \nu_0\,\mathrm{rot}\,\boldsymbol{M} \tag{1}$$

(2) $$E = V_0 - RI_0 - \frac{d\Psi}{dt} = 0$$

(3) $$\boldsymbol{J}_0 = \frac{n_c}{S_c} I_0 \boldsymbol{n}$$

where ν is the reluctivity, $\boldsymbol{J}_0$ is the excitation current density, ν_0 is the reluctivity of the vacuum, $\boldsymbol{M}$ is the magnetization of the permanent magnet, $\boldsymbol{V}_0$ is the applied voltage, R is the resistance, Ψ is the interlinkage magnetic flux of the excited coil, n_c and S_c are the number of turns and the cross-sectional area of the coil respectively, and n_s is the unit normal vector of the coil's cross section.

Coupled Analysis with Motion Equation

The motion of the mover is described as follows:

(7) $$M\frac{d^2x}{dt^2} + D\frac{dx}{dt} + k_x x = F_x$$

(8) $$M\frac{d^2z}{dt^2} + D\frac{dz}{dt} + k_z z = F_z$$

where M is the mass of the mover, x and z are the displacement of the movers, F_x and F_z are the magnetic force components, k_x and k_z are the spring coefficients, and D is the viscous damping coefficient. The thrust of the mover is calculated using the Maxwell stress tensor method, and is substituted into equations (7) and (8). At each time step, the finite element mesh is refreshed, and the position and velocity of the mover are calculated by solving the above equations of motion. Fig. 3 shows the flowchart for this coupled analysis. Vector control is taken into consideration in this analysis.

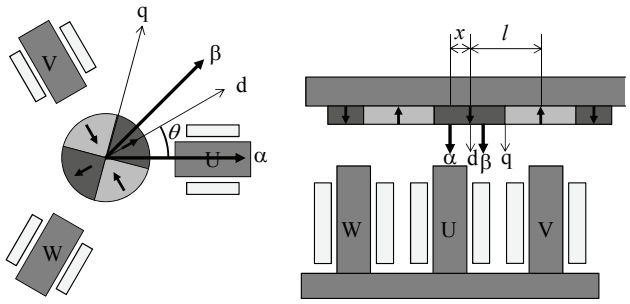

Fig.2. Coordinate system in this actuator

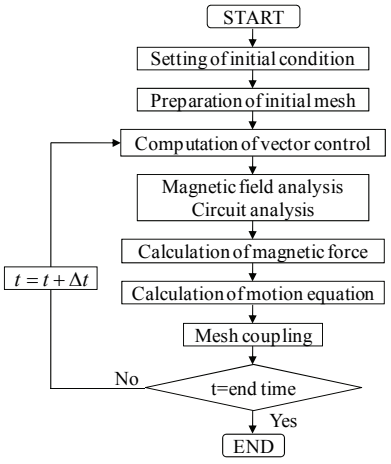

Fig.3 Flowchart for analysis

Analyzed Model and Prototype

Fig. 4 shows the FEM model with the air region omitted. The analyzed region is 1/2 of the whole region because of the symmetry. The number of tetrahedron elements, edges, and unknown variables are 306,400, 367,200, and 347,800, respectively. Table I shows the analysis conditions.

Fig. 5 shows the prototype of this model. Each axis is supported by 2 shafts and a resin bush. The mover can be moved independently on each axis. This prototype is assumed to move with a range of ±1.2mm in the x-direction and ±0.5mm in the z-direction, respectively.

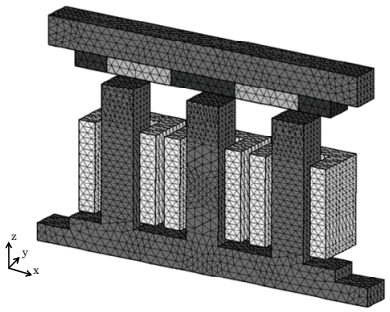

Fig.4. FEM model (1/2 region)

Table 1. Analysis condition

Coils	Maximum voltage (V)	3.6
	Resistance (W)	0.40
	Number of turns (turn)	45
x-axis Mass (g)		48.92
z-axis Mass (g)		24.16
x-axis spring constant (N/mm)		14.70
z-axis spring constant (N/mm)		40.75
Viscous damping coefficient (N·s/m)		0.14

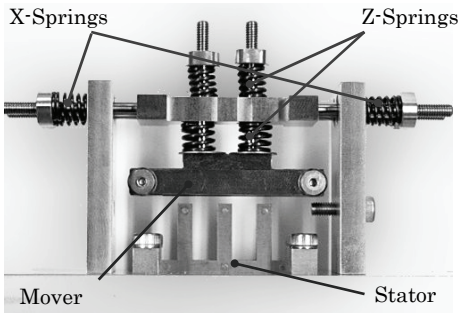

Fig.5. Prototype

Static Characteristics

Fig. 6 shows the analyzed and measured results of the detent thrust when the air-gap is maintained at 1mm. The x-axis component shows good linear characteristics. We can see that the detent force of the calculated results agrees well with the measured results. In the z-axis, although the magnetic attractive force reaches the peak value of 7.6N at the center, it is virtually constant. The absolute value of the experimental data is smaller than that of the calculated results, but qualitatively they agree with each other.

Fig. 7 shows the analyzed and measured results of thrust when each coil was excited at 100A. From these results, thrust with sine-like wave characteristics was obtained. It was found that the z-axis thrust was larger than the x-axis thrust. The measured results are in good agreement with the calculated results.

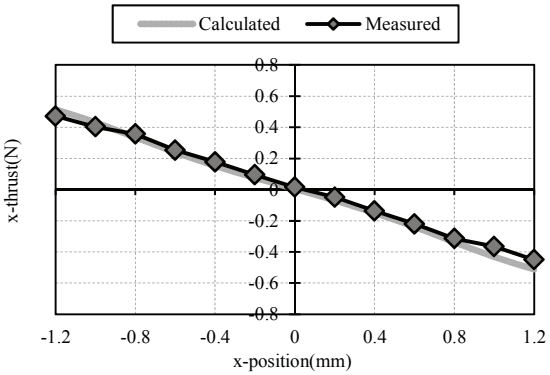

(a) x-axis

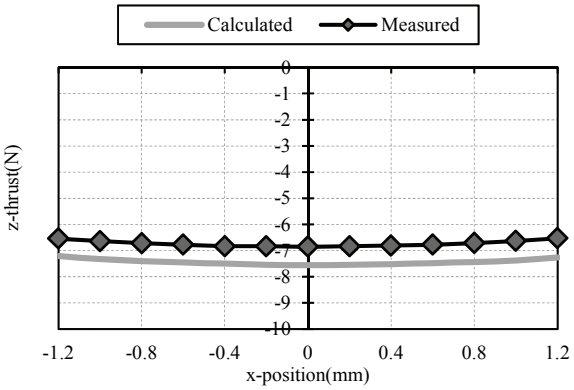

(b) z-axis

Fig.6 Detent characteristics

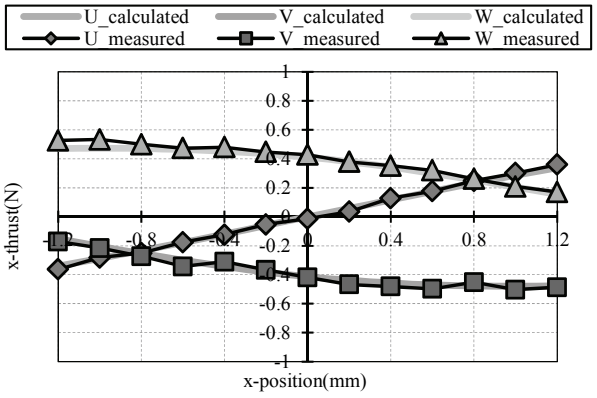

(a)

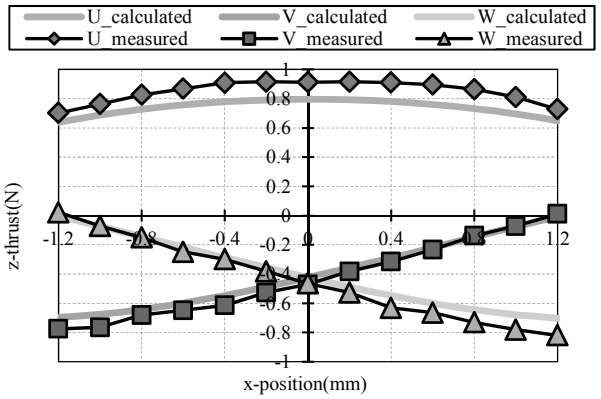

(b) z-axis

Fig.7 Current thrust characteristics

Operation of Prototype Under Vector Control

Figs. 8(a) and (b) show the measured amplitude in the x and z-axes when the actuator was operated to resonate in each axis under vector control. The resonant frequencies of the x and z-axes are 86Hz and 186Hz, respectively. It was found that under vector control, drive in one axis is almost independent of drive in the other. In Fig. 8(a) we can see that there is some vibration in the z-axis during drive in the x-axis. This vibration in z-axis is thought to be due to detent force characteristics. As shown in Fig. 6(b), the detent force of the z-direction changes with displacement of the x-direction and the waveform of the z-axis is distorted by the friction of the resin bush. Fig. 8(c) shows the measured amplitudes of both axes when the actuator was operated to simultaneously resonate in the x and z-axes. As can be seen, the mover can be independently driven in each axis without much large mutual interference.

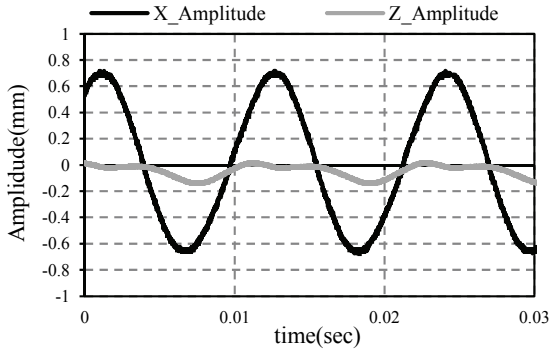

(a) x-axis drive

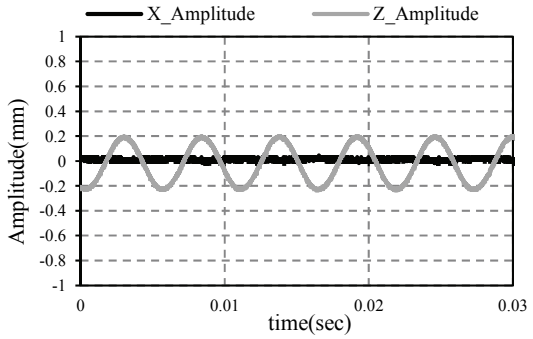

(b) z-axis drive

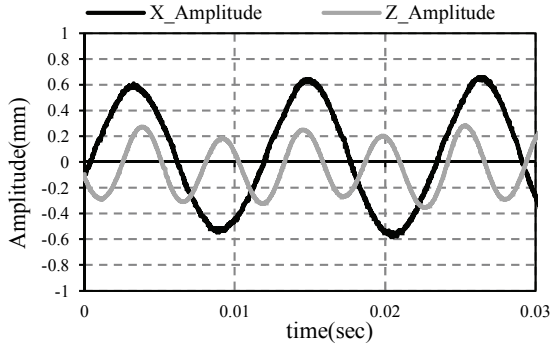

(c) biaxial drive

Fig.8 Experimental results under vector control

Conclusion

In this paper, a new two-DOF resonant actuator with a drive axis in the direction of the air gap under vector control was presented. The static characteristic of the proposed actuator was demonstrated using 3-D FEM analysis and experiments on a prototype. Moreover, from the measurements of the prototype, it was shown that this actuator could be independently driven in the X and Z axes. In the near future, verification of this actuator's dynamic characteristics will be conducted by comparing the empirical data with that from 3-D FEM analysis.

REFERENCES

[1] Y. Asai, K. Hirata, and T. Ota, "Dynamic Analysis Method of Linear Resonant Actuator with Multi-Movers Employing 3-D Finite Element Method", IEEE Trans. Magn., vol.46, no.8, pp.2971-2974, Aug. 2010.

[2] Y. Asai, K. Hirata, and T. Ota, "3-D Finite Element Analysis of Linear Resonance Actuator under PID Control", Proceedings of the 14th Biennial IEEE CEFC (Conference on Electromagnetic Field Computation), 32P8, 2010.

[3] Satoshi Suzuki, Yoshihiro Kawase, Tadashi Yamaguchi, Katsuhiro Hirata and Yu Okaue, "Dynamic Response Analysis of Shear-Type Compact MR Brake", IEEE Trans. Magn., vol.45, no.3, pp.1-4, Mar. 2009.

[4] T. Ota, Y. Mitsutake, Y. Hasegawa, K. Hirata and T. Tanaka, "Dynamic Analysis of Electromagnetic Impact Drive Mechanism Using Eddy Current", IEEE Trans. Magn., vol.43, no.4, pp.1421-1424, 2007.

[5] T. Yamaguchi, Y. Kawase, H. Kodama, K. Hirata, T. Ota and Y. Hasegawa, "Eddy Current Damping Analysis of Laser Marker Using 3-D Finite Element Method", IEEE Trans. Magn., vol.42, no.4, pp.1011-1014, Apr. 2006.

[6] T. Yamaguchi, Y. Kawase, A. Nakase, K. Hirata and T. Ota, "Multi-motion Analysis of Opening and Closing Sensor for Windows Using 3-D Finite Element Method", IEEE Trans. Magn., vol.42, no.4, pp.1015-1018, Apr. 2006.

[7] T. Ota, K. Hirata, T. Yamaguchi, Y. Kawase, K. Watanabe and A. Nakase, "Dynamic Response Analysis of Opening and Closing Sensor for Windows", IEEE Trans. Magn., vol.41, no.5, pp.1604-1607, May. 2005.

[8] Jin, Ping; Fang, Shuhua; Lin, Heyun; Wang, Xianbin; Zhou, Shigui; , "A novel linear and rotary Halbach permanent magnet actuator with two degrees-of-freedom," Journal of Applied Physics , vol.111, no.7, pp.07E725-07E725-3, Apr 2012

[9] Overboom, T.T.; Jansen, J.W.; Lomonova, E.A.; Tacken, F.J.F.; , "Design and Optimization of a Rotary Actuator for a Two-Degree-of-Freedom -Module," Industry Applications, IEEE Transactions on , vol.46, no.6, pp.2401-2409, Nov.-Dec. 2010

[10] T. Yamaguchi, Y. Kawase, S. Suzuki, K. Hirata, T. Ota and Y. Hasegawa "Dynamic Analysis of Linear Resonant Actuator Driven by DC Motor Taking into Account Contact Resistance between Brush and Commutator", IEEE Trans. Magn., vol.44, no.6, pp.1510-1513, Jun. 2008.

[11] Tadashi Yamaguchi, Yoshihiro Kawase, Koichi Sato, Satoshi Suzuki, Katsuhiro Hirata, Tomohiro Ota and Yuya Hasegawa, "Trajectory Analysis of 2-D Magnetic Resonant Actuator" , IEEE Trans. Magn., vol.45, no.3, pp.1732-1735, Mar. 2009.

[12] K. Hirata, T. Yamamoto, T. Yamaguchi, Y. Kawase and Y. Hasegawa, "Dynamic Analysis Method of Two-Dimensional Linear Oscillatory Actuator Employing Finite Element Method", IEEE Trans. Magn., vol.43, no.4, pp.1441-1444, 2007.

***Authors**: Takamichi Yoshimoto, Osaka University, Department of Adaptive Machine Systems, R3-233, 2-1Yamadaoka, Suita, Osaka, 565-0871, Japan, E-mail: takamichi.yoshimoto@ams.eng.osaka-u.ac.jp; Yasuyoshi Asai, Osaka University, Department of Adaptive Machine Systems, R3-233, 2-1Yamadaoka, Suita, 565-0871 Osaka, Japan, E-mail: yasuyoshi.asai@ams.eng.osaka-u.ac.jp; prof. Katsuhiro Hirata Osaka University, Department of Adaptive Machine Systems, R3-233, 2-1Yamadaoka, Suita, Osaka, 565-0871, Japan, E-mail: k-hirata@ams.eng.osaka-u.ac.jp; Tomohiro Ota, Panasonic Electric Works Co., Ltd., Kadoma, Osaka 573-8534, Japan, E-mail: ota.tomorrow@jp.panasonic.com*